

$\text{La}_{0.6}\text{Sr}_{0.4}\text{Co}_{0.2}\text{Fe}_{0.8}\text{O}_3$ as the anode and cathode for intermediate temperature solid oxide fuel cells

A. Hartley*, M. Sahibzada, M. Weston, I.S. Metcalfe, D. Mantzavinos

School of Chemical Engineering, University of Edinburgh, Kings Buildings, Mayfield Road, Edinburgh EH9 3JL, Scotland, UK

Abstract

The perovskite material $\text{La}_{0.6}\text{Sr}_{0.4}\text{Co}_{0.2}\text{Fe}_{0.8}\text{O}_3$ (LSCF-6428) has been considered as both the anode and cathode in solid oxide fuel cells (SOFCs) operating at intermediate temperatures (550–700°C). Solid electrolyte coulometry (SEC) has been used to measure the oxygen non-stoichiometry as a function of temperature and ambient oxygen partial pressure, thus enabling kinetic data relating to oxygen transport in cathodes to be correlated with the material oxygen vacancy concentration. The catalytic activity towards methane oxidation, and susceptibility to deactivation through carbon deposition have both been investigated by temperature programmed methods, and compared with data for the conventional Ni/YSZ anode material. ©2000 Elsevier Science B.V. All rights reserved.

Keywords: Solid oxide fuel cells; Perovskite; Oxygen stoichiometry; Solid electrolyte; Coulometry; Temperature programmed techniques; Methane oxidation

1. Introduction

Fuel cells utilising a solid oxide electrolyte are being developed for clean, efficient energy production. However, the high operating temperatures (typically 800–1000°C) give rise to economic and technical difficulties associated with material property requirements for cell components and balance of plant. Considerable research interest is, therefore, currently directed towards reducing operating temperatures below 700°C, via use of doped ceria-based electrolytes in place of the more conventional yttria-stabilized zirconia (YSZ).

At these intermediate temperatures it has been found that the kinetics of the cathodic reaction tend to limit cell performance [1]. Thus, optimisation of electrode materials and performance is essential. Good candidates for the cathode are perovskite oxides based

upon LaCoO_3 , particularly those substituted with Sr and Fe on A and B sites, respectively. These materials, designated generically as LSCFs, are known to be compatible with ceria-gadolinia electrolytes, to show suitable stability ranges [2], and to possess good conductivity in air at temperatures of interest. Furthermore, the surface oxygen exchange and bulk diffusion characteristics are superior to those of conventional strontium-doped lanthanum manganite (LSM) cathodes [3].

LSCF shows good catalytic activity towards direct methane oxidation [4], and, as a perovskite oxide, may be expected to be less susceptible to deactivation through carbon deposition than traditional Ni/YSZ cermet anode catalysts [5]. Thus, it may also find application on the anode side, provided the stability can be sufficiently controlled.

The use of similar materials for both anode and cathode in the fuel cell would lead to significant advantages in terms of mechanical stability during ther-

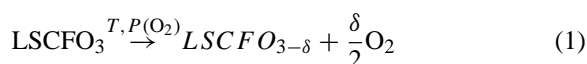
* Corresponding author. Tel.: +44-131-650-4864
E-mail address: anne@chemeng.ed.ac.uk (A. Hartley)

mal cycling. The degree of oxygen non-stoichiometry is a fundamental factor relating many important electrodic properties, including oxygen transport behaviour, electronic conductivity, and catalytic activity. A convenient method of determining the degree of non-stoichiometry (oxygen vacancy concentration) under various conditions of temperature and ambient oxygen partial pressure is, therefore, a pre-requisite for further study, optimisation and control of the material for both anode and cathode. In this study an electrochemical method of stoichiometry determination was developed, and an oxygen pressure/temperature/stoichiometry (p - T - x) diagram established for LSCF-6428 (where the numbers refer to the relative proportions of each constituent, respectively). Temperature programmed techniques were used to investigate the catalytic activity towards methane oxidation and resistance to coking of this composition. Electrochemical techniques may be extended further to yield data on oxygen transport kinetics and material stability ranges. For example, transient re-equilibration data will be used to study the oxygen transport characteristics of the catalyst under various conditions of temperature and $P(\text{O}_2)$, and the limits of catalyst stability will be investigated by a combination of SEC and thermogravimetric techniques.

2. Experimental

2.1. Electrochemical stoichiometry determinations

Solid electrolyte coulometry SEC was used to determine the oxygen non-stoichiometry, δ , for the reaction



The apparatus is a commercially available dual cell and reactor system (Oxylyt) supplied by Sensotech GmbH, and is shown schematically in Fig. 1. Two tubular YSZ cells were operated in series at a constant cell temperature of 700°C. Approximately, 50 mg of powdered sample was placed in a quartz tube reactor between the two solid state cells. An inert gas stream (in this case Research Grade N_2 (BOC)) was passed through Cell 1, over the sample, and finally through Cell 2. In Cell 1, a controlled quantity of oxy-

gen was added to the gas stream via application of a well-defined dosing current. Cell 2 measures the oxygen partial pressure ($P(\text{O}_2)$) of the resulting gas stream according to the Nernst equation

$$V = \frac{RT}{4F} \ln \frac{P(\text{O}_2)}{P(\text{O}_2)_{\text{ref}}} \quad (2)$$

where $P(\text{O}_2)_{\text{ref}}$ is the oxygen partial pressure of the surrounding atmosphere (air), V is the open-circuit cell voltage of Cell 2 and T is the cell temperature (K). Alternatively, Cell 2 may be operated by holding its voltage at a constant value less than that of open circuit, thus allowing a current to pass. In this case, changes in the gas stream $P(\text{O}_2)$, i.e. those due to oxygen release by the sample, can be sensitively and continuously monitored via the cell current at Cell 2, giving rise to an effective titration of the excess oxygen produced by the sample reaction.

It is well known that LSCF-6428 is stoichiometric ($\delta=0$) at temperatures below about 600°C in air [6]. By temperature ramping from room temperature to a target temperature T in a gas stream of defined $P(\text{O}_2)$ therefore, it is possible to monitor continuously the current variation in Cell 2. The quantity of oxygen Q released by the sample during the time interval t_1 to t_2 is then given by

$$Q = \frac{1}{4F} \int_{t_1}^{t_2} (I_t - I_0) dt \quad (3)$$

where I_t is the current at time t , and I_0 is the baseline current prior to the sample reaction.

2.2. Temperature programmed methane oxidation

Powder samples of around 100 mg were placed on a quartz wool bed inside a quartz tube reactor. The tube was connected to gas supplies with stainless steel compression fittings (Swagelok) using graphite ferrules (SGE) to ensure an airtight seal. Gases (BOC) were introduced into the system via 1/8" nylon tubing with flow rates controlled by Tylan mass flow controllers. The output gas stream was analysed by quadrupole mass spectrometer (QMS). The reactor was electrically heated, with power supplied through a control unit connected to a thermocouple placed against the inner wall of the reactor, close to the sample.

For temperature programmed methane oxidation, a 1:1 mixture of CH_4 and O_2 in a He carrier gas

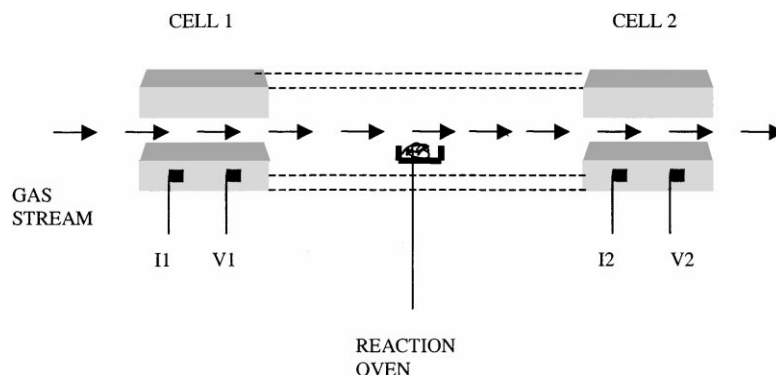


Fig. 1. Schematic diagram of solid electrolyte coulometry apparatus.

was fed to the reactor, and the temperature ramped at 10°C/min. The LSCF catalyst (in powder form) was pre-conditioned in 20% O₂/balance He for 1 h at 600°C. The Ni/YSZ catalyst was formed from a 1:1 mixture of NiO and YSZ powders, wet-milled overnight to form a physical mixture, and subsequently dried. The resulting powder was then reduced in 20% H₂/balance N₂ for 1 h at 600°C before use. The latter procedure was sufficient to ensure full reduction of NiO to metallic Ni. Full reduction was verified via mass loss measurements and also by evaluation of hydrogen consumption.

2.3. Methane decomposition

An indication of the degree of carbon formation was obtained by reacting dry methane over powdered catalyst samples (~50 mg), and analysing the output gas stream by QMS. Catalyst deactivation can be inferred from changes in the decomposition rate. The gas composition used was 30% CH₄ in N₂ carrier and the temperature was ramped at 10°C/min. Deactivation due to carbon deposited on the catalyst surface was assessed via temperature programmed oxidation (TPO) techniques, after completion of the temperature programmed methane oxidation.

2.4. Transient measurements using SEC

A similar technique to that described in Section 2.1 was also used to record transient re-equilibration data for LSCF-6428. In this case a small temperature step change (10°C) was imposed upon a sample previously

in equilibrium with the ambient conditions. This results in a perturbation from equilibrium stoichiometry. Progress towards re-equilibration can then be monitored via the Cell 2 current as before. It is clear from Eq. (3) that data in the form of a fractional weight change as a function of time can readily be obtained, since

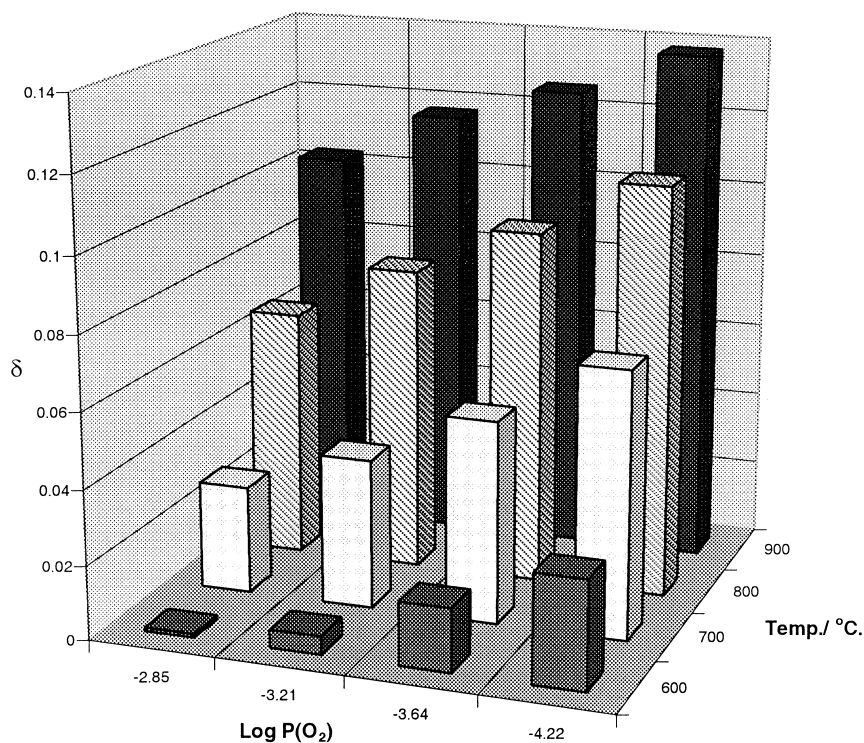
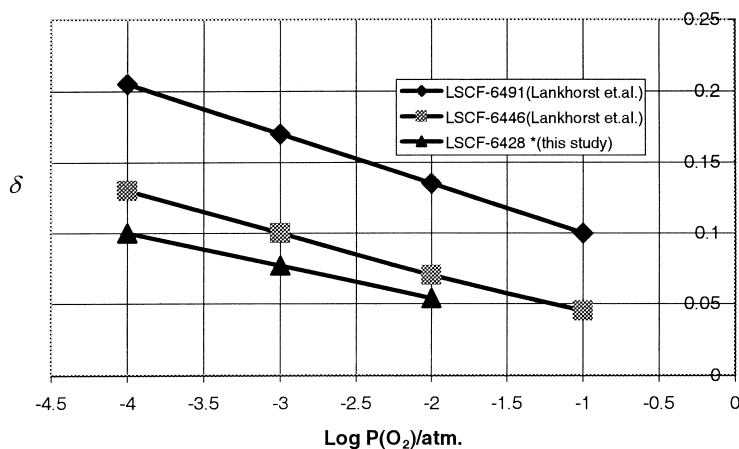
$$\frac{W(t)}{W(\infty)} = \frac{\int_{t=0}^t (I_t - I_0) dt}{\int_{t=0}^{t=\infty} (I_t - I_0) dt} \quad (4)$$

where $W(t)$ represents the weight change at time t , and I_t and I_0 are the values of the measurement cell current at time t and at equilibrium, respectively.

3. Results and discussion

3.1. Stoichiometry determination

Fig. 2 shows the p - T - δ diagram for LSCF-6428 in the range 600–900°C, $\log P(\text{O}_2) = -2.85$ to -4.22 atmospheres. The degree of oxygen non-stoichiometry δ increases with decreasing ambient oxygen partial pressure, and with increasing temperature. The relationship between δ and $\log P(\text{O}_2)$ is approximately linear in this range, and shows excellent consistency with results reported by Lankhorst et al. for LSCF-6446 and LSCF-6491 (SEC methods) [7], and also with results reported by Stevenson et al. for LSCF-6428 in air (TGA methods) [6]. Fig. 3 compares data from this study with Lankhorst's data, showing clearly that δ decreases with increasing Fe/Co ratio as expected. It has been proposed by Lankhorst et al. [7] that the onset of decomposition for these perovskites occurs

Fig. 2. P - T - δ diagram for LSCF-6428.Fig. 3. Nonstoichiometry of LSCF-64 y (1- y) for $y=9, 4$ and 2 , at 800°C.

at, or near, $\delta = 1/2 [\text{Sr}'_{\text{La}}]$, (where $[\text{Sr}'_{\text{La}}]$ indicates the proportion of Sr atoms on La sites, according to standard Kroger–Vink notation) i.e., at $\delta = 0.2$ in the case of LSCF-6428. For the full range of conditions described in Fig. 2, δ is much less than 0.2, and phase stability has, therefore, been assumed.

3.2. Temperature programmed methane oxidation

Fig. 4 shows the activities of Ni/YSZ and LSCF-6428 catalysts towards methane oxidation, in terms of the quantity of CO₂ produced by the reaction. Both materials show comparable activities over

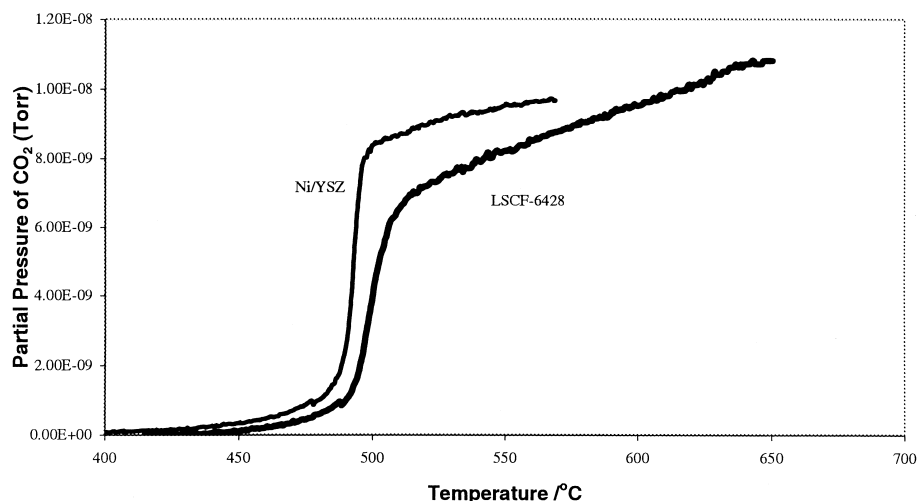


Fig. 4. Comparison of activity towards methane oxidation.

the temperature range of interest with Ni/YSZ appearing only slightly more active at lower temperatures ($<600^{\circ}\text{C}$). With no catalyst present, no reaction is seen until the temperature reaches $\sim 850^{\circ}\text{C}$.

3.3. Susceptibility towards deactivation by carbon formation

Onset of methane decomposition occurs at $\sim 740^{\circ}\text{C}$ for LSCF-6428 (cf. $\sim 400^{\circ}\text{C}$ for Ni/YSZ), as shown by Fig. 5. The LSCF catalyst is significantly more active towards methane decomposition at temperatures above $\sim 820^{\circ}\text{C}$. Methane decomposition may lead to carbon deposition on the catalyst surface, although in the case of oxide catalysts, catalyst reduction may result in the formation of some CO_2 in place of deposited carbon. In this case the rate of reaction continues to increase with temperature, indicating that little deactivation is occurring.

In the case of Ni/YSZ, the reaction rate decreases at higher temperatures suggesting that carbon deposition is affecting the catalyst function, or alternatively that nickel sintering is taking place, thus reducing the active surface area. If significant nickel sintering has occurred, then a subsequent similar run (performed after carbon re-oxidation) should show a reduction in activity. Such a reduction was not observed during a second, or even a third TPRx experiment, though it

could be induced if the catalyst was subjected to very harsh sintering conditions (several hours at 900°C in the presence of water). It can be concluded, therefore, that for this type of powder sample, under the conditions of the experiments described, nickel sintering was not a critical factor. Carbon deposition, on the other hand, was clearly shown to be present, by subsequent temperature programmed oxidation (TPO), (Fig. 6).

The temperature programmed reaction (Fig. 5) was also performed using an LSCF-6428 catalyst which had been pre-reduced in 10% H_2 in N_2 . In this case onset of methane decomposition occurred earlier than for unreduced LSCF, i.e. at $\sim 600^{\circ}\text{C}$, and activity was also higher than for the non-preconditioned sample up to a temperature of $\sim 875^{\circ}\text{C}$. It should be noted, however, that the gas atmosphere used to pre-condition the LSCF catalyst in this case may have been sufficiently reducing in nature to induce some phase instability (i.e., some degree of breakdown of the perovskite structure into its constituent oxides – see Section 3.1). It is interesting to note, in this context, that Xu et al. [8] report phase instability of LSCF-6428 in a pure methane atmosphere at temperatures above about 750°C . However, these authors also observe that low concentrations of oxygen in the methane stream are sufficient to prevent the catalyst reduction.

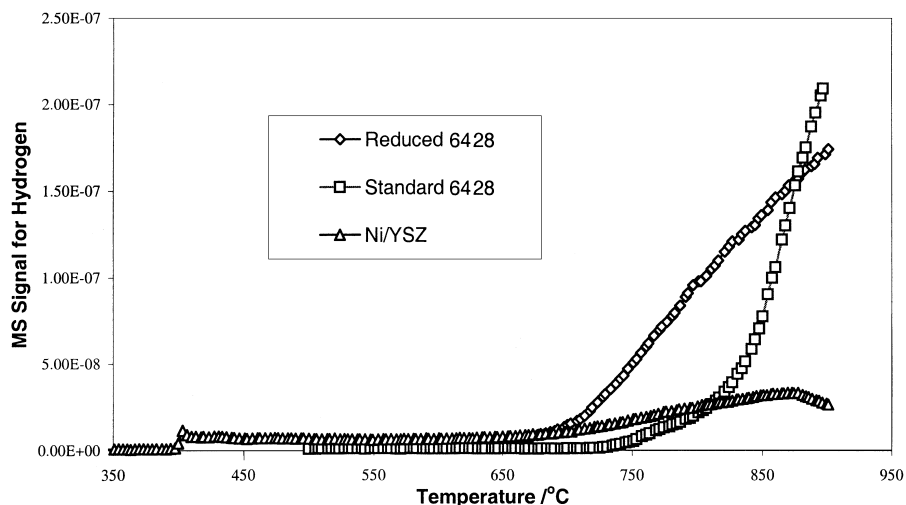


Fig. 5. Comparison of the susceptibility of anode materials towards deactivation by carbon formation.

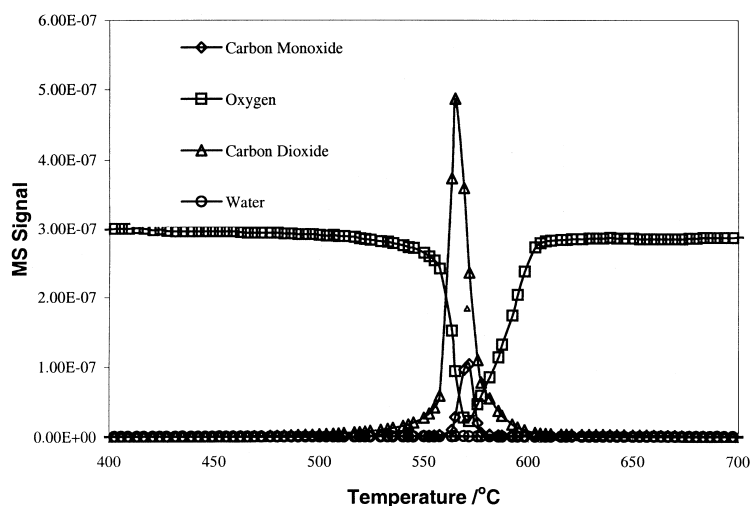
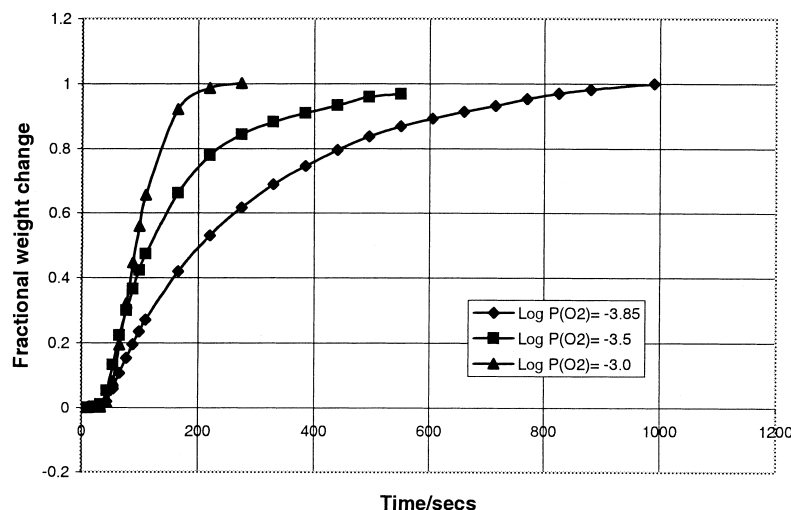
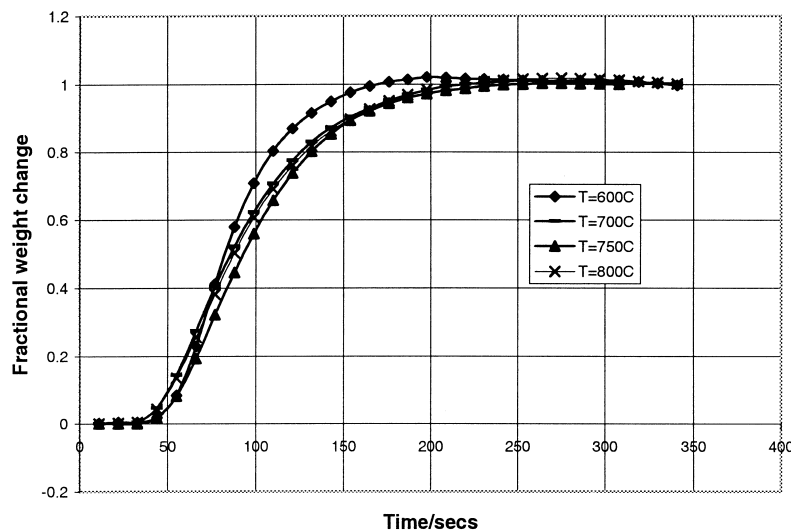


Fig. 6. TPO over Ni/YSZ following exposure to CH_4 .

3.4. Transient re-equilibration measurements

Transient curves representing $W(t)/W(\infty)$ as a function of time were obtained over a range of starting temperatures (600–800°C) and oxygen pressures ($\log P(\text{O}_2) = -2.89$ to -3.85), and hence for a range of different equilibrium stoichiometries in the catalyst. At a temperature of around 750°C, the time to re-equilibration increases by almost a factor of 4 as $\log P(\text{O}_2)$ decreases from -3 to -3.85 (Fig. 7). This corresponds to a change in δ from ~ 0.055 to

~ 0.08 , i.e. oxygen release is slower at higher values of δ (higher oxygen vacancy concentrations in the material). Changes in re-equilibration time for temperatures between 600 and 850°C at constant $P(\text{O}_2)$ (Fig. 8) are considerably less marked. Although δ again increases considerably as temperature is increased (slowing oxygen release) this will be offset to some degree by the thermal effect of the increased temperature on the oxygen mobility within the material. The balance is such that for a given $P(\text{O}_2)$, re-equilibration appears to be most rapid at 600°C (for

Fig. 7. Re-equilibration transient (oxygen release) at $T = 750^{\circ}\text{C}$.Fig. 8. Re-equilibration transient (oxygen release); $\log P(\text{O}_2) = -3.0$.

the range $600\text{--}850^{\circ}\text{C}$). Kinetic information of this type is important for optimising the oxygen transport characteristics of the cathode.

4. Conclusions

The degree of non-stoichiometry of LSCF-6428 has been determined for various temperatures, and for a range of reduced oxygen partial pressures which simulate the working catalyst state under cathodic bias.

This information enables kinetic data to be directly related to the material state, thus facilitating cathode optimisation.

Catalytic activity towards methane oxidation has been demonstrated, together with good resistance to deactivation by carbon deposition. However, phase instability may prove to be an important factor on the anode side at very low $P(\text{O}_2)$ and/or higher temperatures. Further work is required to determine the limits of stability of the material, and to assess the effects of phase instability on longer-term anode performance.

References

- [1] M. Sahibzada, B.C.H. Steele, K. Zheng, R.A. Rudkin, I.S. Metcalfe, *Catal. Today* 38 (1997) 459–466.
- [2] H.U. Anderson, L.-W. Tai, C.C. Chen, M.M. Nasrallah, W. Huebner, *Proceedings of 4th International Symposium On Solid Oxide Fuel Cells (SOFC IV)*, New Jersey, 1995, pp. 375–384.
- [3] J.E. ten Elshof, M.H.R. Lankhorst, H.J.M. Bouwmeester, *Solid State Ionics* 99 (1997) 15–22.
- [4] H.M. Zheng, Y. Shimizu, Y. Teraoka, N. Miura, N. Yamazoe, *J. Catal.* 121 (1990) 432–440.
- [5] R.T. Baker, I.S. Metcalfe, *Appl. Catal., A: General* 126 (1995) 297–317.
- [6] J.W. Stevenson, T.R. Armstrong, R.D. Carneim, L.R. Pederson, W.J. Weber, *J. Electrochem. Soc.* 143 (1996) 2722–2729.
- [7] M.H.R. Lankhorst, J.E. ten Elshof, *J. Solid State Chem.* 130 (1997) 302–310.
- [8] S.J. Xu, W.J. Thomson, *Ind. Eng. Chem. Res.* 37 (1998) 1290–1299.